Short, Strong Hydrogen Bonds on Enzymes: NMR and Mechanistic Studies

ARTICLE *in* JOURNAL OF MOLECULAR STRUCTURE · SEPTEMBER 2002

Impact Factor: 1.6 · DOI: 10.1016/S0022-2860(02)00212-0

ELSEVIER

Journal of Molecular Structure 615 (2002) 163–175

Journal of
MOLECULAR
STRUCTURE

www.elsevier.com/locate/molstruc

Short, strong hydrogen bonds on enzymes: NMR and mechanistic studies

A.S. Mildvan[a,*], M.A. Massiah[a], T.K. Harris[a], G.T. Marks[b], D.H.T. Harrison[b], C. Viragh[c], P.M. Reddy[c], I.M. Kovach[c]

[a]*Department of Biological Chemistry, The Johns Hopkins University School of Medicine, 725 North Wolfe Street, Baltimore, MD 21205, USA*
[b]*Department of Biochemistry, Medical College of Wisconsin, 8701 Watertown Plank Road, Milwaukee, WI 53226, USA*
[c]*Department of Chemistry, The Catholic University of America, Washington, DC 20064, USA*

Received 5 September 2001; accepted 8 October 2001

Abstract

The lengths of short, strong hydrogen bonds (SSHBs) on enzymes have been determined with high precision (±0.05 Å) from the chemical shifts (δ), and independently from the *D*/*H* fractionation factors (ϕ) of the highly deshielded protons involved. These H-bond lengths agree well with each other and with those found by protein X-ray crystallography, within the larger errors of the latter method (±0.2 to ± 0.8 Å) [Proteins 35 (1999) 275]. A model dihydroxynaphthalene compound shows a SSHB of 2.54 ± 0.04 Å based on $\delta = 17.7$ ppm and $\phi = 0.56 \pm 0.04$, in agreement with the high resolution X-ray distance of 2.55 ± 0.06 Å. On ketosteroid isomerase, a SSHB is found (2.50 ± 0.02 Å), based on $\delta = 18.2$ ppm and $\phi = 0.34$, from Tyr-14 to the 3-O^- of estradiol, an analog of the enolate intermediate. Its strength is ~7 kcal/mol. On triosephosphate isomerase, SSHBs are found from Glu-165 to the 1-NOH of phosphoglycolohydroxamic acid (PGH), an analog of the enolic intermediate (2.55 ± 0.05 Å), and from His-95 to the enolic-O^- of PGH (2.62 ± 0.02 Å). In the methylglyoxal synthase–PGH complex, a SSHB (2.51 ± 0.02 Å) forms between Asp-71 and the NOH of PGH with a strength of ≥4.7 kcal/mol. When serine proteases bind mechanism-based inhibitors which form tetrahedral Ser-adducts analogous to the tetrahedral intermediates in catalysis, the Asp···His H-bond of the catalytic triad becomes a SSHB [Proc. Natl Acad. Sci. USA 95 (1998) 14664], 2.49–2.63 Å in length. Similarly, on the serine-esterase, butyrylcholinesterase complexed with the mechanism-based inhibitor *m*-(*N*,*N*,*N*-trimethylammonio)-2,2,2-trifluoroacetophenone, a SSHB forms between Glu-327 and His-438 of the catalytic triad, 2.61 ± 0.04 Å in length, based on $\delta = 18.1$ ppm and $\phi = 0.65 \pm 0.10$. Very similar results are obtained with (human) acetylcholinesterase. The strength of this SSHB is at least 4.9 kcal/mol.

Keywords: Short, strong hydrogen bonds; Phosphoglycolohydroxamic acid; Nucleic acids

1. Introduction

Short, strong hydrogen bonds (SSHBs) ranging in length from 2.45 to 2.65 Å, have been detected by NMR methods in several enzymes by four criteria: (i) the presence of highly deshielded proton resonances (15–20 ppm), (ii) the *D*/*H* fractionation factors of

* Corresponding author. Tel.: +1-410-955-2038; fax: +1-410-955-5759.
E-mail address: mildvan@welchlink.welch.jhu.edu (A.S. Mildvan).

0022-2860/02/$ - see front matter
PII: S0022-2860(02)00212-0

such protons are significantly lower than 1.0, (iii) the solvent exchange rates of these protons are slowed by at least an order of magnitude, (iv) such hydrogen bonds are *at least* 5 kcal/mol in strength, as determined by pH titration or by the effects of mutations on kinetic parameters of the enzyme [1–3]. These properties of SSHBs contrast sharply with those of normal, weak hydrogen bonds, which predominate in proteins and nucleic acids [4,5], and which are 2.7–3.0 Å in length, and 2 ± 1 kcal/mol in strength.

It is important to make the fine distinction between a SSHB and a normal, weak hydrogen bond because SSHBs, when present, usually participate directly in catalysis, and the strengths of hydrogen bonds increase sharply with decreasing length between 2.7 and 2.4 Å [6]. The small differences in length between normal hydrogen bonds and SSHBs generally preclude this distinction being made by protein X-ray crystallography, where the errors in mean atomic positions are 0.1–0.3 times the resolution [2,7] and protons are only rarely detected. Hence, in an otherwise satisfactory 2.0 Å X-ray structure of a protein, the uncertainties in hydrogen bond lengths range from ±0.2 to ± 0.6 Å, depending on the local noise level. For this reason, it was necessary to develop more precise methods in order to make this distinction [1–3]. NMR has provided two methods which give precise (±0.05 Å) and accurate hydrogen bond distances: the chemical shift (δ), and the *D*/*H* fractionation factor (ϕ) of the proton involved [1–3]. This paper will review the properties and mechanistic roles of SSHBs in enzymes, which were established by the above NMR criteria.

2. Experimental

2.1. General NMR methods

Proton NMR spectra were collected on a Varian Unity Plus 600 MHz spectrometer using a Varian 5 mm triple resonance probe and the 1331 pulse sequence [8] to avoid water excitation. NMR samples (0.6 ml) contained 0.3–1.0 mM enzyme sites in dilute buffer, pH 7.5 (10 mM sodium phosphate + 20 mM NaCl with ketosteroid isomerase; 20 mM Tris-d_{11}–HCl + 100 mM NaCl with triosephosphate isomerase; 20 mM Tris-d_{11}–HCl with methylglyoxal synthase; 50 mM sodium phosphate with butyryl- and acetylcholinesterases). With ketosteroid isomerase [9] and triosephosphate isomerase [10], where it was necessary to lower the sample temperature to −5 °C to minimize exchange broadening of the hydrogen bonded proton resonances, 10% (v/v) DMSO-d_6 was added to prevent sample freezing and to provide a strong signal for field/frequency locking. In the other cases, where proton exchange was slow at 25–30 °C, DMSO was not required, and 10% (v/v) D_2O was added for field/frequency locking.

Exchange rates of hydrogen bonded protons with solvent, or their upper limits, were determined by the temperature dependence of $1/T_2$, as measured by the resonance widths at half height, permitting estimation of the exchange rate protection factors [1].

2.2. Determination of hydrogen bond lengths from proton chemical shifts

As hydrogen bonds shorten, proceeding from weak to strong, the proton becomes less electronically shielded, resulting in a downfield shift of its resonance, approaching a maximum value of 21 ppm [1–3,11]. The mechanism of this deshielding is a slight lengthening of the covalent A–H moiety of the A–H···B hydrogen bond, which attenuates the major shielding provided by the sigma bonding electron pair. Other diamagnetic effects on chemical shifts are at least an order of magnitude smaller.

For O–H···O hydrogen bonds, the measured chemical shift (δ) is used to calculate the full hydrogen bond distance (D) with Eq. (1)

$$D(\mathrm{O{-}H{\cdots}O}) = 5.04 - 1.16\ln(\delta) + 0.0447(\delta) \quad (1)$$

Eq. (1) was obtained empirically [12] by fitting a wide range of 59 O–H···O hydrogen bond lengths, measured by small molecule high resolution X-ray diffraction, with chemical shifts (δ) determined by solid state NMR in the same crystals [11].

For imidazolium$^+$–carboxylate$^-$ (N–H$^+$···O$^-$) hydrogen bonds, a correlation of 12 full hydrogen bond distances (D), obtained by small molecule high resolution X-ray diffraction, with chemical shifts (δ) determined by solid state NMR in the same crystals [13] is well fit empirically by Eq. (2), which may be used to determine imidazolium$^+$–carboxylate$^-$ (N–H$^+$···O$^-$)

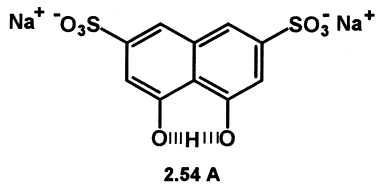

Scheme 1.

hydrogen bond lengths [14,15]

$$D(\mathrm{N{-}H^{+}\cdots O^{-}}) = 1.99 + 0.198\ln(\delta) + (10.14/(\delta))^{5} \quad (2)$$

From Eqs. (1) and (2), it can be shown that a proton is more deshielded in an imidazolium^{+}–carboxylate^{-} N–H$^{+}\cdots$O^{-} hydrogen bond than in an O–H$\cdots$O hydrogen bond of the same length. Thus, in a hydrogen bond 2.65 Å in length, the proton chemical shift is 15.6 ppm for an imidazolium^{+}–carboxylate^{-} interaction and 12.9 ppm for an O–H$\cdots$O interaction. The additional 2.7 ppm deshielding in the imidazolium^{+}–carboxylate^{-} hydrogen bond likely results from a slight lengthening of the covalent N–H bond and to a much lesser extent from the aromatic ring current effect of the imidazolium cation.

2.3. Determination of hydrogen bond lengths from fractionation factors

The *D*/*H* fractionation factor of a molecule (ϕ) is defined as the equilibrium constant for the exchange of deuterium from the solvent into a protonated site on the molecule. For a site on an enzyme, this equilibrium constant may be written as follows:

$$\phi = [\mathrm{Enz} - D][H_{solvent}]/[\mathrm{Enz} - H][D_{\mathrm{solvent}}] \quad (3)$$

Thus, ϕ measures the preference of this site for deuterium over protium, relative to solvent. As discussed elsewhere [1–3,16], because the zero point vibrational energy of a deuteron in a hydrogen bond decreases less than that of a proton, the presence of a deuteron in a hydrogen bond is disfavored relative to a proton, resulting in a $\phi < 1.0$. The shorter and stronger the hydrogen bond, the lower the fractionation factor, minimizing at a ϕ value of 0.16 at an O–H$\cdots$O hydrogen bond distance of 2.39 Å [17]. At shorter hydrogen bond lengths, a very strong single well O$\cdots$H$\cdots$O hydrogen bond exists in which ϕ increases with decreasing length [17]. The fractionation factor provides a measure of the distance (Δx_{min}) between the two free energy wells of a hydrogen bond in which the proton may be located (Eq. (4))

$$\mathrm{A{-}H\cdots B} \rightleftarrows \mathrm{A\cdots H{-}B} \quad (4)$$

The distance (in Å) between the proton wells (Δx_{min}) over the range 0.397–0.685 Å may be obtained directly from the measured ϕ value using a published nomograph [1–3,18] which is based on assumed quartic potential functions for both *H* and *D* [17], or equivalently, from the third order polynomial fit of Eq. (5)

$$(\Delta x_{\mathrm{min}}) = 0.2220 + 1.1924(\phi) - 1.3347(\phi)^{2} + 0.6080(\phi)^{3} \quad (5)$$

which gives the same Δx_{min} values as the nomograph, within error. Adding two covalent bond lengths (typically 2.00 Å) to Δx_{min} yields a measurement of the hydrogen bond length, assuming the hydrogen bond to be linear. Bent hydrogen bonds would result in shorter hydrogen bond lengths. The use of Eq. (5) assumes the energy levels of the two proton wells to be equal. If the energy levels were unequal, the hydrogen bond length would be shorter. Thus ϕ values yield hydrogen bond distances, or their upper limits, which are needed to establish SSHBs.

Fractionation factors (ϕ) for proton resonances are determined by varying the H_2O/D_2O content of the solvent allowing sufficient time for equilibration to occur, measuring the integrated resonance intensities (I), and fitting the data to Eq. (6) [1–3,19]

$$I = [I_{\mathrm{max}}(X)]/[\phi(1 - X) + X] \quad (6)$$

In Eq. (6), X is the mole fraction H_2O and I_{max} the peak integral at 100% H_2O.

3. Results and discussion

3.1. Model studies

We have previously reported low temperature proton NMR studies of aqueous sodium 4,5-dihydroxynaphthalene-2,7-disulfonate (Scheme 1) which contains a short, strong O–H$\cdots$O hydrogen bond [3,

Table 1
Hydrogen bond lengths in a model compound and on isomerase and lyase enzymes derived from proton chemical shifts (δ), fractionation factors (ϕ), and X-ray crystallography

System	Interaction	δ (ppm)	ϕ	Hydrogen bond length (Å) from			
				δ	ϕ	X-ray	Error range in X-ray[a]
4,5-DHND[b]	O–H···O	17.7[c]	0.56 ± 0.04	2.50 ± 0.02	2.57 ± 0.01	2.55[d]	±0.06
KSI–DHE[e]	H100···E77	13.1[f]	0.79 ± 0.09[f]		2.64 ± 0.03	2.75[g]	0.25–0.75
	Y14···$^{-}$O–C	18.2[f]	0.34 ± 0.02[f]	2.49 ± 0.02	2.50 ± 0.01	2.58[h]	0.25–0.75
	D99···$^{-}$O–C	11.6[f]	0.97 ± 0.08[f]	2.72 ± 0.02	2.68 ± 0.02	2.62[h]	0.25–0.75
TIM–PGH[i]	E165···HON	14.9[j]	0.38 ± 0.06[j]	2.57 ± 0.05	2.52 ± 0.02	2.68, 3.08[k]	0.19–0.57
	H95···O=C	13.5[j]	0.71 ± 0.02[j]		2.62 ± 0.01	2.66, 3.12[k]	0.19–0.57
MGS–PGH[l]	D71···HON	18.1[m]	0.43 ± 0.02[m]	2.49 ± 0.02	2.53 ± 0.01	2.30–2.36[m]	0.24
	H98···O=C	13.8[m]	1.18 ± 0.05[m]		>2.75	2.77–2.85[m]	0.24

[a] Standard error range in Å is 0.1–0.3 times the resolution [2,3,7], or the error in mean atomic position from a Luzzati plot.
[b] Sodium 4,5-dihydroxynaphthalene-2,7-disulfonate.
[c] From Ref. [9].
[d] Average ± SD of 22 small molecule X-ray structures of dihydroxynaphthalene derivatives from the Cambridge Data Bank.
[e] Ketosteroid isomerase complex of dihydroequilenin.
[f] From Ref. [12].
[g] From Ref. [51].
[h] From Ref. [26].
[i] Triosephosphate isomerase complex of phosphoglycolohydroxamic acid.
[j] From Ref. [10].
[k] From Ref. [49].
[l] Methylglyoxal synthase complex of phosphoglycolohydroxamic acid.
[m] From Ref. [34].

9] analogous to the short, strong N–H···N hydrogen bonds found in diaminonaphthaline compounds or 'proton sponges' [20]. The deshielded chemical shift (δ) of 17.7 ppm of the O–H···O proton in the dihydroxynaphthalene compound yielded, from Eq. (1) a hydrogen bond length of 2.50 ± 0.02 Å [3]. We have recently determined the *D*/*H* fractionation factor (ϕ) of this proton to be 0.56 ± 0.04 which yields from Eq. (5) a distance between the two proton wells (Δx_{min}) of 0.57 ± 0.01 Å. Adding two covalent bond lengths yields a hydrogen bond distance of 2.57 ± 0.01 Å. These hydrogen bond distances obtained from NMR and their average, 2.54 ± 0.04 Å agree closely with the average (± the standard deviation) of 2.55 ± 0.06 Å found for 22 high resolution small molecule X-ray structures of dihydroxynaphthalene derivatives in the Cambridge data bank (Table 1) [3]. An additional model is provided by the imidazolium^{+}–carboxylate^{-} N–H···O interaction in the catalytic triad of subtilisin. This hydrogen bond length is 2.63 ± 0.04 Å from the proton chemical shift of 17.4 ppm, using Eq. (2) and 2.56 ± 0.01 Å from its ϕ value of 0.53 ± 0.02 (Table 2). These distances, and their average, 2.60 ± 0.04 Å agree with the value of 2.62 ± 0.08 Å obtained from an unusually high resolution X-ray structure (0.78 Å) of subtilisin [21].

3.2. Ketosteroid isomerase

Ketosteroid isomerase, the first isomerase enzyme in which a SSHB or 'low barrier hydrogen bond' was detected [9], catalyzes the conversion of Δ^5- to Δ^4-3-ketosteroids (Fig. 1) using Asp-38 as a general base [22], and both Tyr-14 [22] and Asp-99 [23] as general acids. Asp-99 has an unusually high pK_a > 9 [24], because of its location in a hydrophobic environment with a low local dielectric constant of ~18 [25] and its proximity to Asp-38. The acid catalysts act either separately (Fig. 1(A)) [23], or as a catalytic diad (Fig. 1(B)) [12]. The mechanism of Fig. 1(A) is consistent with the 2.5 Å X-ray structure of the enzyme,

Table 2
Hydrogen bond lengths in serine proteases derived from proton chemical shifts (δ), fractionation factors (ϕ), and X-ray crystallography

System	Interaction	δ (ppm)	ϕ	Hydrogen bond length (Å) from			
				δ[a]	ϕ	X-ray	Error range in X-ray[b]
H^+-Chymotrypsinogen	H57···D102	18.1[c]	0.40 ± 0.02[c]	2.62 ± 0.04	2.52 ± 0.01	2.63, 2.65[d]	0.18–0.54
H^+-Chymotrypsin	H57···D102	18.2[e]	0.64 ± 0.02[e]	2.61 ± 0.04	2.60 ± 0.01	2.61, 2.65[f]	0.17–0.50
Chymotrypsin–BoroPhe[g]	H57···D102	16.9[e]	0.65 ± 0.01[e]	2.63 ± 0.04	2.60 ± 0.01	2.70[h]	0.18–0.54
Chymotrypsin–*N*-AcF–CF_3[i]	H57···D102	18.6[j]	0.32 ± 0.01[j]	2.61 ± 0.04	2.49 ± 0.01	2.61[k]	0.15
Chymotrypsin–*N*-AcLF–CF_3[l]	H57···D102	18.9[j]	0.43 ± 0.20[j]	2.61 ± 0.04	2.53 ± 0.08	2.61[k]	0.15
Subtilisin–BoroPhe[g]	H64···D32	17.4[e]	0.53 ± 0.02[e]	2.63 ± 0.04	2.56 ± 0.01	2.62[m]	0.20–0.60
Subtilisin–sAAPF[n]	H64···D32					2.62[o]	0.08–0.24

[a] The His^+-Asp^- distances from δ were obtained from Eq. (2) [13–15].
[b] Standard error range in Å is 0.1–0.3 times the resolution [2,3,7], or the error in mean atomic position from a Luzzati plot.
[c] From Ref. [52].
[d] From Ref. [53].
[e] From Ref. [18].
[f] From Ref. [54].
[g] BoroPhe is methoxysuccinyl-Ala-Ala-*Pro*-2-amino-3-phenylethylboronic acid.
[h] Chymotrypsin complex with phenylethane boronic acid [55].
[i] *N*-AcF-CF_3 is *N*-acetyl-L-phenylalanyl-trifluoromethyl ketone.
[j] From Ref. [41].
[k] From Ref. [48].
[l] *N*-AcLF-CF_3 is *N*-acetyl-L-leucyl-L-phenylalanyl-trifluoromethyl ketone.
[m] Subtilisin complex with D-*p*-chlorophenyl-1-acetamido boronic acid [56].
[n] sAAPF is succinyl-alanyl-alanyl-prolyl-phenylalanine.
[o] From Ref. [21].

complexed with dihydroequilenin, an analog of the dienolate intermediate [26], and with the additive effects on k_{cat} of mutations of Tyr-14 and Asp-99 [27]. The mechanism of Fig. 1(B) is supported by the loss in the Y14F mutant of the hydrogen bonded proton resonances of *both* Tyr-14 and Asp-99 (see below) [9,12], and by the solution structure of ketosteroid isomerase complexed with 19-nortestosterone hemisuccinate, a product analog and substrate of the reverse isomerase reaction [28]. However, the solution structure cannot exclude the mechanism of Fig. 1(A) [28].

Low temperature proton NMR revealed the appearance of two deshielded resonances in complexes of the enzyme with analogs of the dienolic intermediate, estradiol and dihydroequilenin, one at 18.15 ppm and the other at 11.60 ppm [9,12]. However the precise assignment of these two signals to Tyr-14 and Asp-99 was uncertain because the single mutation of Tyr-14 to Phe (Y14F) abolished *both* resonances [9,12,29], an observation consistent with the mechanism of Fig. 1(B). Recently, several mutations of Asp-99 were reported [23,29,30], the most revealing of which was the Asp-99-Leu mutant which abolished only the 11.60 ppm resonance and preserved the 18.15 ppm signal [29], establishing the assignment of the deshielded 18.15 ppm signal to Tyr-14 as we had originally suggested [9], and the 11.60 ppm signal to the carboxyl proton of Asp-99 (Fig. 1). Table 1 and Fig. 1 correct these assignments which were reversed in Refs. [1–3,12]. The length of the hydrogen bond from Tyr-14 to the 3-O^- of the dienolate analog is 2.49 ± 0.02 Å from its chemical shift [9], 2.50 ± 0.01 Å from its fractionation factor of 0.34 ± 0.02 [1–3], and 2.58 ± 0.23 Å from the 2.3 Å X-ray structure [29] (Table 1). The strength of this SSHB has been found by three independent methods to be $\geq$7 kcal/mol [9,22,31]. Mutational studies suggest that Tyr-14 contributes a factor of $10^{4.7}$ to catalysis [9], consistent with a SSHB.

The resonance at 11.60 ppm, with a typical chemical shift for a carboxyl proton, is now assigned to Asp-99–COOH in a normal hydrogen bond (Fig. 1) with lengths of 2.72 ± 0.02, 2.68 ± 0.02, and

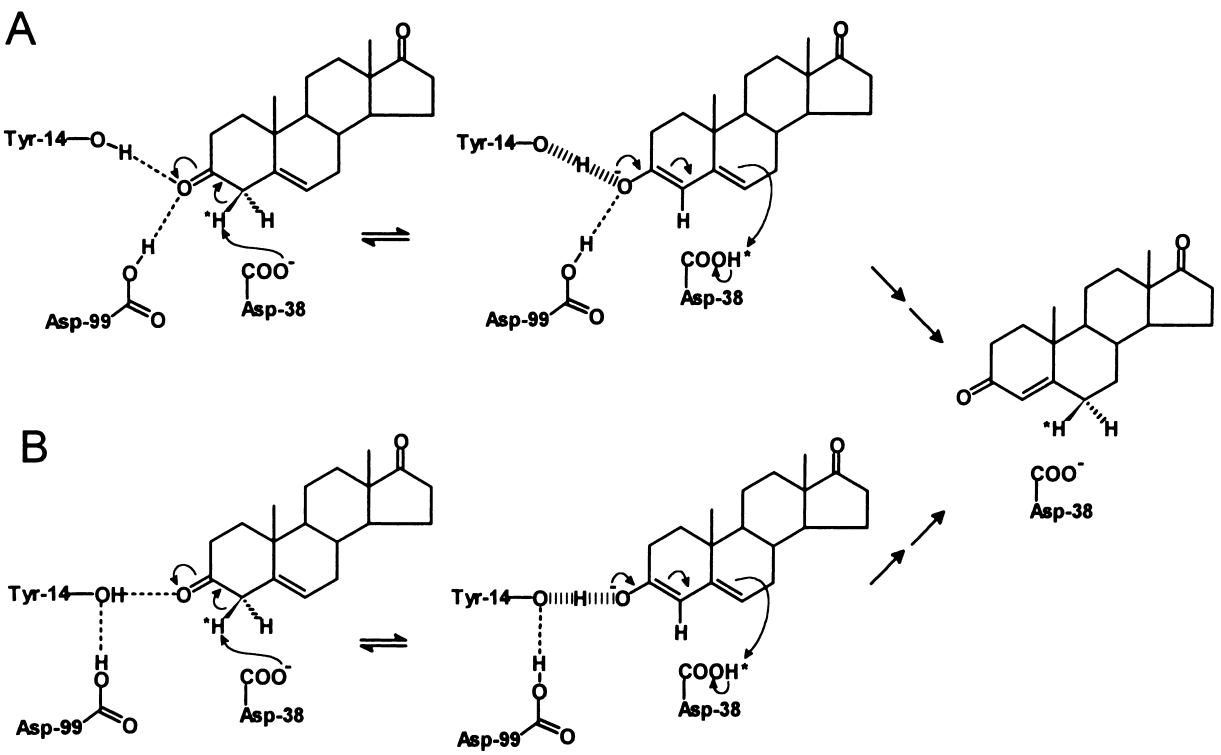

Fig. 1. Revised alternative mechanisms for the Δ^5-3-ketosteroid isomerase reaction showing a SSHB from Tyr-14 to the 3-O^- of the dienolate intermediate. In (A) the intermediate is stabilized by separate hydrogen bonds from Tyr-14 and Asp-99 [23,26,27,29]. In (B) the intermediate is stabilized by a catalytic diad: Asp-99 to Tyr-14 to the intermediate [2,3,9,12].

2.62 ± 0.24 Å from its chemical shift, its fractionation factor of 0.97 ± 0.08 [12], and the X-ray structure [26], respectively. Mutational studies suggest that Asp-99 contributes a factor of 10^2–$10^{3.5}$ to catalysis [23,30], consistent with a normal hydrogen bond.

3.3. Triosephosphate isomerase and methylglyoxal synthase

While these two enzymes share neither sequence nor structural similarities, the reactions they catalyze are similar in that both initially convert dihydroxyacetone phosphate (DHAP) to a *cis*-enediolic intermediate (Fig. 2). On triosephosphate isomerase (TIM), this enediolic intermediate results from the abstraction of the *pro-R* C3 proton of DHAP by Glu-165, facilitated by polarization of the C2 carbonyl group of DHAP by His-95 [10,32,33]. On methylglyoxal synthase this enediolic intermediate results from the abstraction of the *pro-S* C3 proton of DHAP by Asp-71, facilitated by polarization of the C2 carbonyl group of DHAP by His-98 [34]. Triosephosphate isomerase then catalyzes proton donation to the C2 carbon of the enediolic intermediate to form D-glyceraldehyde phosphate, while methylglyoxal synthase catalyzes the elimination of phosphate from the same enediolic intermediate to form the enol of methylglyoxal (Fig. 2).

On triosephosphate isomerase, we have previously found that phosphoglycolohydroxamic acid (PGH), an analog of the enediolic intermediate, formed two SSHBs with the enzyme (Fig. 3(A)), one between His-95 NεH and the C2 carbonyl group of PGH (2.62 ± 0.01 Å), and the other between Glu-165 and the NOH of PGH (2.55 ± 0.05 Å) (Table 1) [2,3,10]. During catalysis, with the true enediolic intermediate, the former SSHB would facilitate C2 carbonyl polarization, while the catalytic role of the latter SSHB between Glu-165 and PGH–NOH is not clear. It may

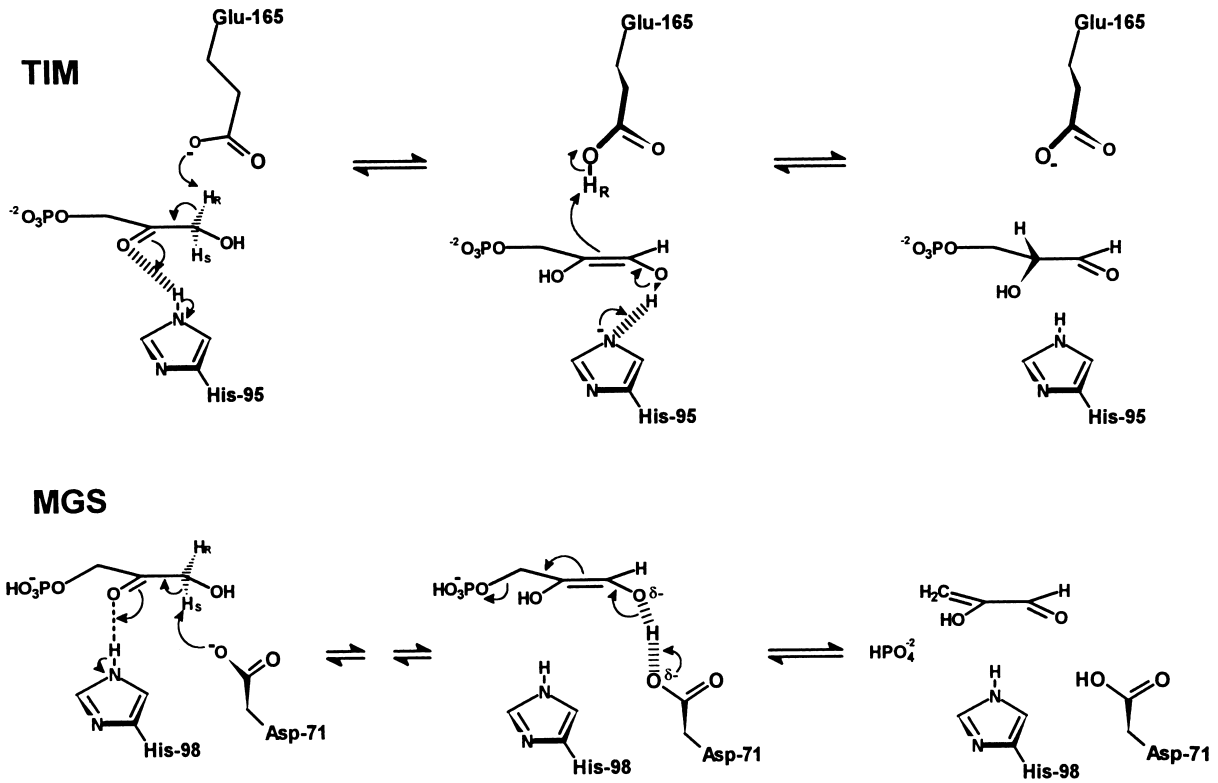

Fig. 2. Comparison of the mechanisms of the reactions of DHAP catalyzed by triosephosphate isomerase (TIM) [10,32,33], and by methylglyoxal synthase (MGS) [34], showing the roles of SSHBs.

function merely to help bind the intermediate tightly and thereby lower its free energy. Alternatively or additionally, this SSHB might participate in proton transfer from O3 to C2 of the intermediate in a criss-cross mechanism, which is believed to occur in the H95Q mutant [35], and which may also contribute to catalysis in the wild type enzyme [10,33,36]

In the reaction catalyzed by methylglyoxal synthase (MGS), the role of such a SSHB (from PGH–NOH to Asp-71) would be clear because the 3-OH of the enediolic intermediate must be deprotonated during the elimination of phosphate (Fig. 2). Kinetic analysis showed PGH to be an unusually tight-binding competitive inhibitor of methylglyoxal synthase with a K_I (39 nM) which was $10^{2.2}$-fold tighter than that found with triosephosphate isomerase, suggesting that PGH was functioning as an analog of the transition state rather than of the intermediate on methylglyoxal synthase [34]. The high affinity of methylglyoxal synthase for PGH might be due in part to a SSHB between the enzyme and the ligand.

The X-ray structure of the methylglyoxal synthase homohexamer, complexed with PGH, at 2.0 Å resolution detected a hydrogen bond from PGH–NOH to the carboxylate of Asp-71 with lengths ranging from 2.30 to 2.37 ± 0.24 Å in the six subunits of the homohexamer [34]. Proton NMR showed a PGH-dependent deshielded resonance at 18.1 ppm with a *D*/*H* fractionation factor $\phi = 0.43 \pm 0.02$, yielding more precise hydrogen bond lengths of 2.49 ± 0.02 and 2.53 ± 0.01 Å, respectively, for the SSHB from PGH–NOH to the carboxylate of Asp-71 (Table 1) [34]. The strength of this SSHB is estimated to be at least 4.7 kcal/mol, based on the $10^{3.5}$-fold decrease in k_{cat} of the D71N mutant [37], although the kinetics of this multi-step reaction are complex.

^{15}N NMR of MGS-bound PGH showed a large 14 ppm deshielding of N3 indicating a significant

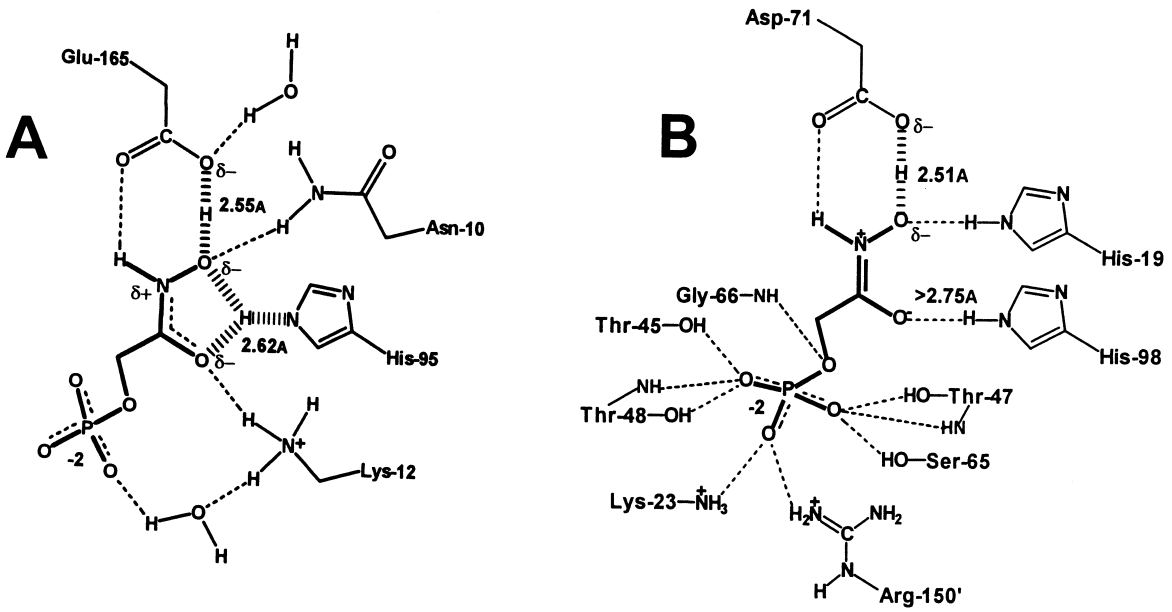

Fig. 3. Structures, based on NMR and X-ray studies, of the phosphoglycolohydroxamic acid (PGH) complexes of (A) triosephosphate isomerase [10,49,50], and of (B) methylglyoxal synthase [34] showing SSHBs.

imidate resonance contribution to the structure of the bound ligand with a partial positive charge on the nitrogen, a partial N3=C2 double bond, and polarization of the C2 carbonyl group (Fig. 3(B)). From the X-ray structure, His-98, in the plane of PGH, donates a normal hydrogen bond from its NεH to the C2–O^- of PGH with lengths ranging from 2.77 to 2.85 ± 0.24 Å in the six subunits. A proton resonance at 13.8 ppm with a fractionation factor of 1.18 ± 0.05 is assigned to the NεH of neutral His-98 [34]. Based on the fractionation factor exceeding unity, a normal, weak hydrogen bond is indicated, with a length exceeding 2.75 Å, the hydrogen bond length in ice (Table 1) [38].

In the X-ray structure, the phosphate of MGS-bound PGH, corresponding to the leaving group of the enediolic intermediate, accepts nine hydrogen bonds, 2.45–3.22 ± 0.24 Å in length, from seven residues (Fig. 3(B)), and is tilted out of the imidate plane of PGH toward the *re* face (Fig. 2) [34]. Since Asp-71 approaches the NOH of PGH on the same *re* face, both Asp-71 and phosphate are appropriately positioned, stereoelectronically, to function as base and leaving group, respectively, in a concerted, suprafacial 1,4-elimination of phosphate from the enediolic intermediate in the second step of the methylglyoxal synthase reaction (Figs. 2 and 4). Another active site residue, His-19, approaches the *si* face of PGH, donating a normal, weak hydrogen bond from its NεH to the NOH oxygen of the ligand with lengths ranging from 2.93 to 3.10 ± 0.24 Å in the six subunits. A proton resonance at 12.1 ppm with a fractionation factor 1.10 ± 0.07 is assigned to the NεH of neutral His-19 [34]. The ϕ value exceeding unity indicates a hydrogen bond length greater than 2.75 Å.

Although alternative mechanisms for methylglyoxal synthase cannot be excluded, the data suggest that Asp-71 is the single base that initially abstracts the *pro-S* proton from DHAP, and subsequently the 3-OH proton from the enediolic intermediate via a SSHB, as shown in the detailed mechanism of Fig. 4 [34]. Phosphate departure is facilitated by the above mentioned nine hydrogen bonds to this leaving group.

3.4. Serine proteases and serine esterases

These enzymes share similar active sites consisting of a substrate binding region which determines specificity, an oxyanion hole, and a catalytic triad which promote the hydrolysis. The hydrogen-bonded catalytic triad consists of Asp···His···Ser in serine proteases and Glu···His···Ser in cholinesterases. In

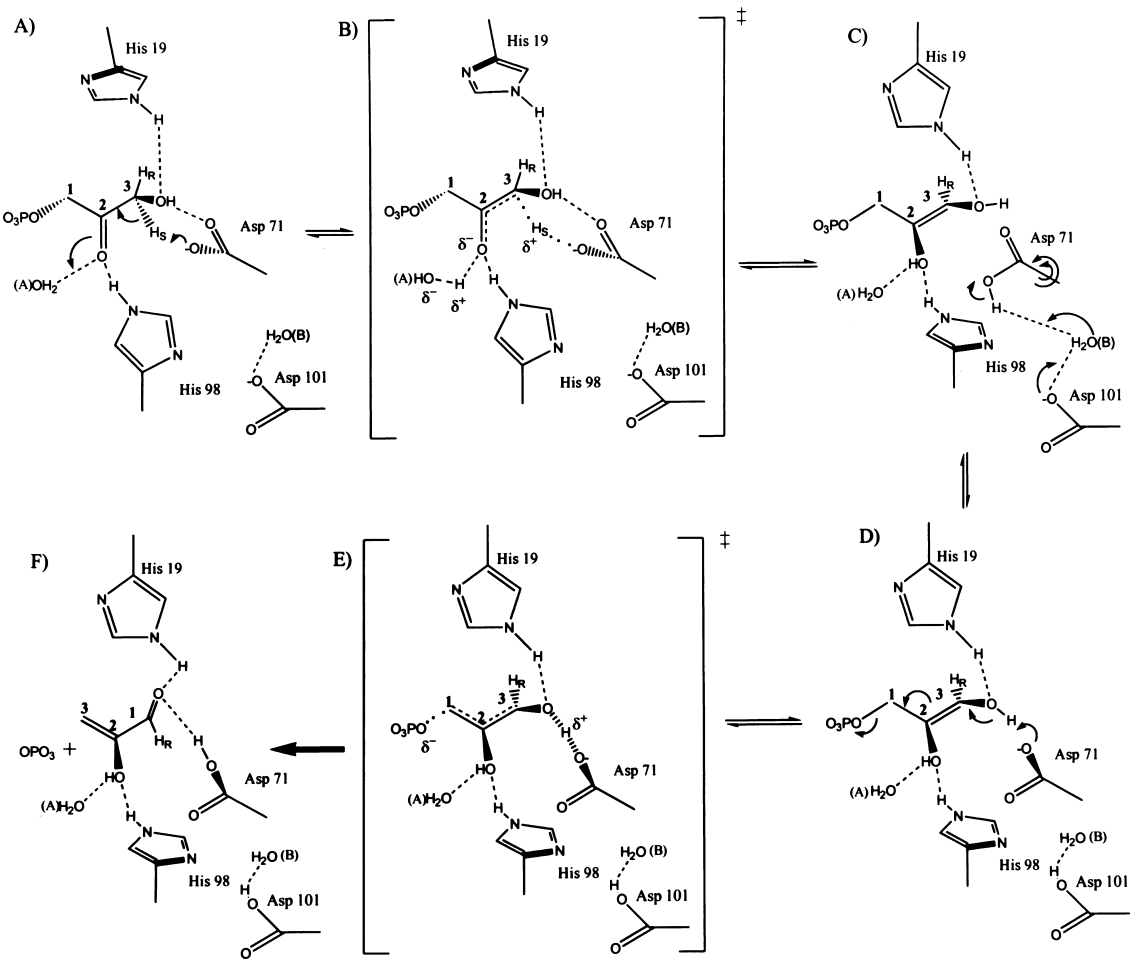

Fig. 4. Proposed mechanism of the methylglyoxal synthase reaction based on X-ray and NMR studies of the MGS–PGH complex [34].

the reaction mechanisms, the His residue, aided by the Asp (or Glu) residue, acts as a general base, deprotonating the catalytic serine for nucleophilic attack at the substrate carbonyl group, which is polarized by the residues of the oxyanion hole, yielding a tetrahedral intermediate. Next, the His NεH^+ acts as a general acid, protonating the departing amine (or alcoholate) (Figs. 5 and 6). The resulting acyl-serine enzyme intermediate is then hydrolyzed by a water molecule, in a similar mechanism, to regenerate free enzyme for the next catalytic cycle.

Upon binding mechanism-based inhibitors which form tetrahedral adducts that resemble the tetrahedral intermediate, or at low pH, when the His is cationic, serine proteases form a SSHB between the Asp^- and His-NδH^+ of the catalytic triad [18,39–41]. This is shown by the appearance of a deshielded proton resonance (16.9–18.9 ppm) with a low fractionation factor (0.32–0.64) (Table 2). The hydrogen bond lengths for serine proteases derived from chemical shifts using Eq. (2) range from 2.61 to 2.63 Å, and those derived from fractionation factors using Eq. (5) range from 2.49 to 2.60 Å, in good agreement with each other and with corresponding measurements from X-ray crystallography. However, the distances determined by protein crystallography have much larger errors, with the exception of the 0.78 Å resolution X-ray structure of the subtilisin complex of a mechanism-based inhibitor which yielded an unusually precise SSHB length of 2.62 ± 0.08 Å

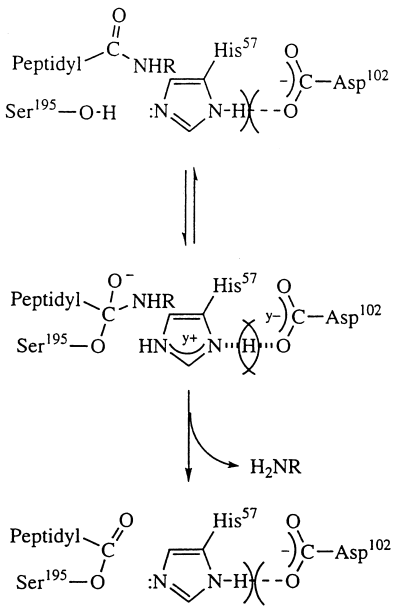

Fig. 5. Mechanism of the acylation half-reaction catalyzed by chymotrypsin utilizing a SSHB between Asp-102 and the cationic form of His-57 [40,41].

(Table 2) [21]. The strength of the SSHB in chymotrypsin has been estimated to be ~7 kcal/mol, the effect of which is to increase the pK_a of the catalytic His from 6.5 to 12 [40].

Cholinesterases, which accelerate ester hydrolysis by ~10^{13}-fold, are more powerful enzymes than serine proteases which accelerate peptide hydrolysis by only ~10^{10}-fold. The interactions of mechanism-based inhibitors with equine butyrylcholinesterase (BChE) [14] or with human acetylcholinesterase (AChE) [15] result in the appearance of deshielded proton resonances (15.5–18.1 ppm) with low fractionation factors (0.47–0.76) (Table 3), indicating the formation of a SSHB between Glu and His NδH of the catalytic triad (Fig. 6). Hydrogen bond distances of 2.62–2.65 Å are obtained from δ, and 2.55–2.63 Å from ϕ. These distances agree closely with each other and with distances obtained by X-ray structures of AChE from *T. californica*, although the errors in the latter distances are much greater (Table 3).

With AChE, the fractionation factors measured by NMR for the SSHB from the His NδH to the Glu of the catalytic triad in analogs of the tetrahedral intermediate [15], agree with transition state fractionation factors for both the acylation and deacylation reactions measured by solvent deuterium kinetic isotope effects [42–45]. The kinetically determined ϕ values are for the proton in flight from the catalytic Ser (and from H_2O) to the His Nε during the acylation (and deacylation) steps, respectively. This agreement in fractionation factors for protons interacting with *both* Nδ and Nε of the catalytic His indicates that the effect of the SSHB between Glu and the Nδ of His is

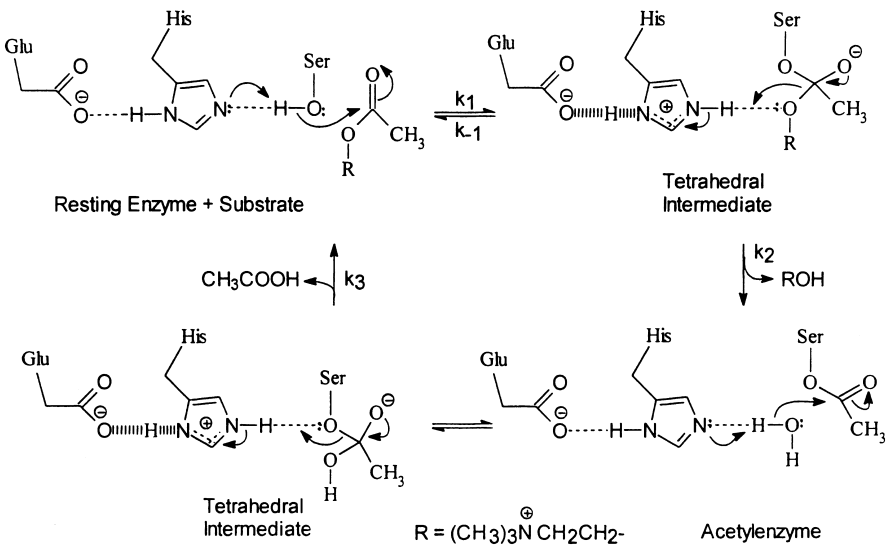

Fig. 6. Mechanism of cholinesterases showing the participation of SSHBs in the tetrahedral intermediates of the acylation and deacylation reactions of the catalytic serine [14,15].

Table 3
Hydrogen bond lengths in the serine esterases butyrylcholinesterase (BChE) and acetylcholinesterase (AChE) derived from proton chemical shifts (δ), fractionation factors (ϕ), and X-ray crystallography

System	Interaction	δ (ppm)	ϕ	Hydrogen bond length (Å) from			
				δ[a]	ϕ	X-ray	Error range in X-ray[b]
BChE-TMTFA[c]	H440···E327	18.1[d]	0.63 ± 0.10[d]	2.62 ± 0.04	2.59 ± 0.03	2.66[e]	0.28–0.84
BChE-paraoxon[f]	H440···E327	16.1[d]	0.72 ± 0.10[d]	2.64 ± 0.04	2.62 ± 0.02	2.60[g]	0.22–0.66
AChE-TMTFA[c]	H440···E327	17.8[h]	0.76 ± 0.10[h]	2.62 ± 0.02	2.63 ± 0.03	2.66[e]	0.28–0.84
AChE-paraoxon[f]	H440···E199	15.5[h]	–	2.65 ± 0.02	–	2.64[i]	0.22–0.66
H^+AChE	H440···E327	16.6[h]	–	2.63 ± 0.02	–	2.60[g]	0.22–0.66
	H440···E199	16.4[h]	–	2.63 ± 0.02	–	3.64[j]	0.25–0.75
	H440···E327	17.7[h]	–	2.62 ± 0.02	–	2.52[j]	0.25–0.75
AChE-NPMP[k]	H440···E199	15.8[h]	0.49 ± 0.10[h]	2.65 ± 0.02	2.56 ± 0.03	2.64[i]	0.22–0.66
	H440···E327	16.5[h]	0.47 ± 0.10[h]	2.63 ± 0.02	2.55 ± 0.03	2.60[g]	0.22–0.66

[a] The His^+-Glu^- distances from δ were obtained from Eq. (2) [13–15].
[b] Standard error range in Å is 0.1–0.3 times the resolution [2,3,7].
[c] Enzyme complex of TMTFA, (*m*-(*N*,*N*,*N*-trimethylammonio)trifluoroacetophenone).
[d] From Ref. [14].
[e] AChE complex of TMTFA, (*m*-(*N*,*N*,*N*-trimethylammonio)trifluoroacetophenone) [47].
[f] Aged enzyme complex of paraoxon (4-nitrophenyl diethylphosphate).
[g] Aged AChE-adduct of soman, (2-(3,3-dimethylbutyl)methylphosphonofluoridate) [57].
[h] From Ref. [15].
[i] Initial AChE-adduct of VX, (*O*-ethyl-*S*-{2-[bis(1methylethyl)amino]ethyl}-methylphosphonothioate) in which a hydrogen bond from His-440-NδH to Glu-199 is detected [58].
[j] Free AChE, pH 5.8. The hydrogen bond from His-440-NδH to Glu-199 is not detected by X-ray [47].
[k] Aged AChE adduct of NPMP (4-nitrophenyl 2-propyl methylphosphonate).

transmitted across the imidazole ring to Nε in the transition state, facilitating proton abstraction from Ser (and from water) in the acylation (and deacylation) steps, respectively (Fig. 6). The strength of the SSHB between Glu and His is estimated to be at least 4.9 kcal/mol on the basis of the ≥3150-fold decrease in activity of the Glu-to-Ala mutant [46]. A contribution of Glu to catalysis of this magnitude could result from its increasing the pK_a of the catalytic His by at least 3.5 units to a value ≥10, more closely approaching that of the Ser to be deprotonated [15].

The lengths of the SSHBs found in cholinesterases overlap with those found in serine proteases (Table 1) indicating that the 10^3-fold greater catalytic powers of cholinesterases do not result from differences in hydrogen bonding in their catalytic triads. One possible structural explanation for the greater catalytic powers of cholinesterases over serine proteases is a difference in the oxyanion hole, which consists of *three* backbone NH hydrogen bond donors in cholinesterases [47], and only *two* in serine proteases, the effects of which may be weak [48].

With AChE, formation of the serine ethyl phosphate diester (with paraoxon) or the serine methylphosphonate diester (with 4-nitrophenyl 2-propyl methylphosphonate) resulted in the appearance of *two* slowly exchanging SSHBs, the summed concentrations of which were approximately stoichiometric with the neutral His-440 (*T. californica* numbering) which was lost (Table 3). Similarly, two slowly exchanging SSHBs were also seen with free AChE at low pH, where His-440 is protonated [15]. The two SSHBs likely result from the slow interchange ($<880\ s^{-1}$) of His-440 NδH between two hydrogen bond acceptors, Glu-327 of the catalytic triad, and the nearby residue Glu-199 (Fig. 7). While too slow to participate in catalysis, which occurs with a k_{cat} of $1.6 \times 10^4\ s^{-1}$, this interchange may contribute to the slow dealkylation of phosphorylated and phosphonylated adducts of the catalytic serine [15].

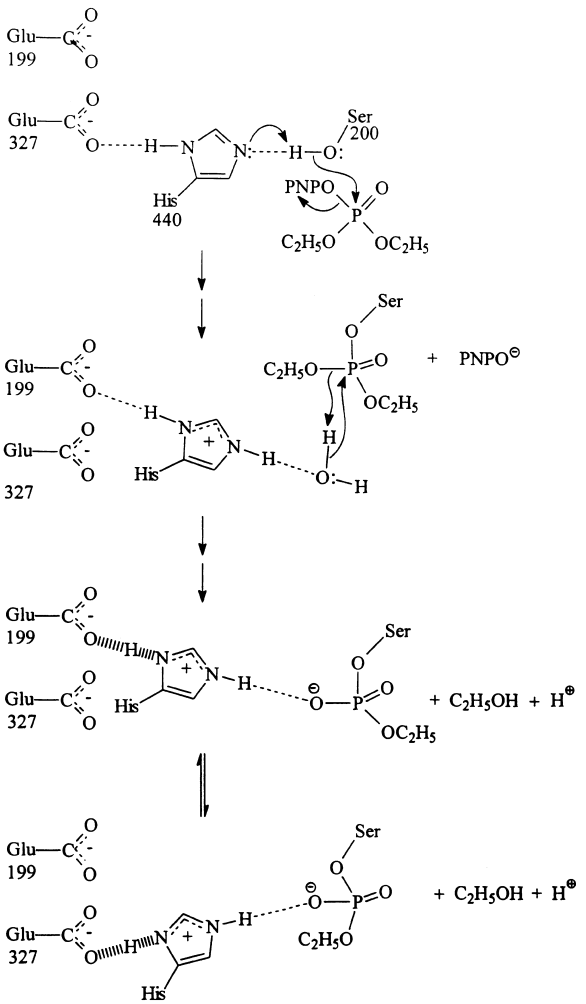

Fig. 7. Mechanisms of phosphorylation of the catalytic serine of acetylcholinesterase by paraoxon and of the subsequent slow dealkylation of the serine-phosphotriester, showing the participation of two SSHBs at the active site [15].

The chemically related internal displacement of diacylglycerol from phosphatidylinositol by phospholipase C to yield D-myoinositol 1,2 cyclic phosphate has recently been shown to make use of a SSHB between His-32 and Asp-274 which promotes the deprotonation of the attacking 2′-OH group of the substrate by His-32 [59]. At pH 6, a deshielded proton resonance is seen ($\delta = 16.4$ ppm) with a fractionation factor $\phi = 0.79 \pm 0.11$, which yield hydrogen bond lengths of 2.63 ± 0.04 and 2.63 ± 0.03 Å, respectively [59], consistent with the X-ray determined distance of 2.6 ± 0.3 Å [60].

Acknowledgments

These studies were supported by National Institutes of Health Grants DK28616 (to A.S.Mildvan), DK07422 (to Paul Talalay), DK51697 (to D.H.T Harrison), and US Army Medical Research and Material Command Contract DAMD17-98-8021 (to I.M. Kovach).

References

[1] A.S. Mildvan, T.K. Harris, C. Abeygunawardana, Meth. Enzymol. 308 (1999) 219.
[2] T.K. Harris, A.S. Mildvan, Proteins 35 (1999) 275.
[3] T.K. Harris, Q. Zhao, A.S. Mildvan, J. Mol. Struct. 552 (2000) 97.
[4] G.I. Makhatadze, P. Privalov, Adv. Prot. Chem. 47 (1995) 307.
[5] J.D. Watson, N.H. Hopkins, J.W. Roberts, J.A. Steitz, A.M. Weiner, Molecular Biology of the Gene, Benjamin/Cummings, Menlo Park, CA, 1987, p. 132.
[6] F. Hibbert, J. Emsley, Adv. Phys. Org. Chem. 26 (1990) 255.
[7] W.N. Lipscomb, in: D.W. Darnall, R.G. Wilkins (Eds.), Methods for Determining Metal Ion Environments in Proteins, Elsevier, New York, 1980, p. 265.
[8] D.L. Turner, J. Magn. Reson. 54 (1983) 146.
[9] Q. Zhao, C. Abeygunawardana, P. Talalay, A.S. Mildvan, Proc. Natl Acad. Sci. USA 93 (1996) 8220.
[10] T.K. Harris, C. Abeygunawardana, A.S. Mildvan, Biochemistry 36 (1997) 14661.
[11] A.E. McDermott, C.F. Ridenour, Proton Chemical Shift Measurement in Biological Solids, Encyclopedia of NMR, Wiley, Sussex, England, 1996, p. 3820.
[12] Q. Zhao, C. Abeygunawardana, A.G. Gittis, A.S. Mildvan, Biochemistry 36 (1997) 14616.
[13] Y. Wei, A.E. McDermott, in: J.C. Facelli, A.C. DeDios (Eds.), Modeling NMR Chemical Shifts: Gaining Insights into Structure and Environment, Oxford University Press, Cary, NC, 1999, p. 177.
[14] C. Viragh, T.K. Harris, P.M. Reddy, M.A. Massiah, A.S. Mildvan, I.M. Kovach, Biochemistry 39 (2000) 16200.
[15] M.A. Massiah, C. Viragh, P.M. Reddy, I.M. Kovach, J. Johnson, T.L. Rosenberry, A.S. Mildvan, Biochemistry 40 (2001) 5682.
[16] M.M. Kreevoy, J. Chem. Educ. 41 (1964) 636.
[17] M.M. Kreevoy, T.M. Liang, J. Am. Chem. Soc. 102 (1980) 3315.
[18] D. Bao, W.P. Huskey, C. Kettner, F. Jordan, J. Am. Chem. Soc. 121 (1999) 4684.
[19] S.N. Lo, J.L. Markley, Biochemistry 33 (1994) 1029.
[20] Z. Malarski, T. Lis, Z. Olejnik, E. Grech, J. Nowicka-Scheibe, I. Majerz, L. Sobczyk, J. Mol. Struct. 552 (2000) 249.
[21] P. Kuhn, M. Knapp, S.M. Soltis, G. Granshaw, M. Thoene, R. Bott, Biochemistry 37 (1998) 13446.

[22] A. Kuliopulos, A.S. Mildvan, D. Shortle, P. Talalay, Biochemistry 28 (1989) 149.
[23] R.W. Wu, S. Ebrahenian, M.E. Zawrotney, L.D. Thornberg, G.C. Perez-Alverado, P. Brothers, R.M. Pollack, M.F. Summers, Science 276 (1997) 415.
[24] L.D. Thornburg, F. Henot, D.P. Bash, D.C. Hawkinson, S.D. Bartel, R.M. Pollack, Biochemistry 37 (1998) 10499.
[25] Y.-K. Li, A. Kuliopulos, A.S. Mildvan, P. Talalay, Biochemistry 32 (1993) 1816.
[26] S.W. Kim, S.-S. Cha, H.-S. Cho, J.-S. Kim, N.-C. Cha, M.-J. Cho, S. Joo, K.K. Kim, K.Y. Choi, B.-H. Oh, Biochemistry 36 (1997) 14030.
[27] R.M. Pollack, L.D. Thornberg, A.R. Wu, M.F. Summers, Arch. Biochem. Biophys. 370 (1999) 9.
[28] M.A. Massiah, C. Abeygunawardana, A.G. Gittis, A.S. Mildvan, Biochemistry 37 (1998) 14701.
[29] H.-S. Cho, N.-C. Ha, G. Choi, H.-J. Kim, D. Lee, K.S. Oh, K.S. Kim, W. Lee, K.Y. Choi, B.-H. Oh, J. Biol. Chem. 274 (1999) 32863.
[30] G. Choi, N.C. Ha, S.W. Kim, D.-H. Kim, S. Park, B-H. Oh, K.Y. Choi, Biochemistry 39 (2000) 903.
[31] L. Xue, P. Talalay, A.S. Mildvan, Biochemistry 30 (1991) 10858.
[32] E.B. Nickbarg, J.R. Knowles, Biochemistry 27 (1988) 5939.
[33] T.K. Harris, R.N. Cole, F.I. Comer, A.S. Mildvan, Biochemistry 37 (1998) 16828.
[34] G.T. Marks, T.K. Harris, M.A. Massiah, A.S. Mildvan, D.H.T. Harrison, Biochemistry 40 (2001) 6805.
[35] E.B. Nickbarg, R.C. Davenport, G.A. Petsko, J.R. Knowles, Biochemistry 30 (1991) 5821.
[36] Q. Cui, M. Karplus, J. Am. Chem. Soc. 123 (2001) 2284.
[37] D. Saadat, D.H.T. Harrison, Biochemistry 37 (1998) 10074.
[38] V.R. Brill, A. Tippe, Acta Crystallogr. 23 (1967) 343.
[39] G. Robillard, R.G. Shulman, J. Mol. Biol. 86 (1974) 541.
[40] C.S. Cassidy, J. Lin, P.A. Frey, Biochemistry 36 (1997) 4576.
[41] J. Lin, W.M. Westler, W.W. Cleland, J.L. Markley, P.A. Frey, Proc. Natl Acad. Sci. USA 95 (1998) 14664.
[42] T.L. Rosenberry, Adv. Enzymol. 43 (1975) 104.
[43] D.M. Quinn, Chem. Rev. 87 (1987) 955.
[44] I.M. Kovach, M. Larson, R.L. Schowen, J. Am. Chem. Soc. 108 (1986) 3054.
[45] J.L. Hogg, J.P. Elrod, R.L. Schowen, J. Am. Chem. Soc. 102 (1980) 2082.
[46] A. Shafferman, C. Kronman, Y. Flashner, M. Leitner, H. Grossfield, A. Ordentlich, Y. Gozes, S. Cohen, N. Ariel, D. Barak, M. Harel, I. Silman, J.L. Sussman, B. Velan, J. Biol. Chem. 267 (1992) 17640.
[47] M. Harel, D.M. Quinn, H.K. Nair, I. Silman, J.L. Sussman, J. Am. Chem. Soc. 118 (1996) 2340.
[48] D. Neidhart, Y. Wei, C. Cassidy, J. Lin, W.W. Cleland, P.A. Frey, Biochemistry 40 (2001) 2439.
[49] R.C. Davenport, P.A. Bash, B.A. Seaton, M. Karplus, G.A. Petsko, D. Ringe, Biochemistry 30 (1991) 5821.
[50] P.J. Lodi, J.R. Knowles, Biochemistry 30 (1991) 6948.
[51] H.-S. Cho, G. Choi, K.Y. Choi, B.-H. Oh, Biochemistry 37 (1998) 8325.
[52] J.L. Markley, W.M. Westler, Biochemistry 35 (1996) 11092.
[53] D. Wang, W. Bode, R.J. Huber, J. Mol. Biol. 185 (1985) 595.
[54] H. Tsukuda, D.M. Blow, J. Mol. Biol. 184 (1985) 703.
[55] A. Tulinsky, R.A. Blevins, J. Biol. Chem. 262 (1987) 7737.
[56] V.S. Stoll, B.T. Eger, R.C. Hynes, V. Martichonok, J.B. Jones, E.F. Pai, Biochemistry 37 (1998) 451.
[57] C.B. Millard, G. Kryger, A. Ordentlich, H.M. Greenblat, M. Harel, M.L. Raves, Y. Segall, D. Barak, A. Shafferman, I. Silman, J.L. Sussman, Biochemistry 38 (1999) 7032.
[58] C.B. Millard, G. Koellner, A. Ordentlich, A. Shafferman, I. Silman, J.L. Sussman, J. Am. Chem. Soc. 121 (1999) 9883.
[59] M. Ryan, T. Liu, F.W. Dahlquist, O.H. Griffith, Biochemistry 40 (2001) 9743–9750.
[60] D.W. Heinz, M. Ryan, T.L. Bullock, O.H. Griffith, EMBO J. (1995) 3855–3863.